

# Accumulation of Simulated Pathological Level of Formaldehyde Decreases Cell Viability and Adhesive Morphology in Neuronal Cells\*

WANG Jing<sup>1)\*\*</sup>, ZHOU Jun<sup>2)\*\*</sup>, MO Wei-Chuan<sup>2)</sup>, HE Ying-Ge<sup>2)</sup>, WEI Yan<sup>2)</sup>, HE Rong-Qiao<sup>2)\*\*\*</sup>, YI Fa-Ping<sup>1)\*\*\*</sup>

<sup>1)</sup> Department of Biochemistry and Molecular Biology, Chongqing Medical University, Chongqing 400016 China;

<sup>2)</sup> State Key Laboratory of Brain and Cognitive Sciences, Institute of Biophysics, Chinese Academy of Sciences, Beijing 100101 China)

**Abstract** Age-related cognitive impairment, for instance Alzheimer's disease (AD), is a chronic, progressive, neurodegeneration disease. The concentration of endogenous formaldehyde (FA) positively correlates with the severity of cognitive impairments in AD patients. However, the FA concentrations used in the previous studies were usually higher than the physiological and pathological levels in aging people. To elucidate the relationship between FA and the pathogenesis of AD, it is necessary to investigate the effect of long-term exposure of neurons to low concentration of FA, which is consistent with the pathological FA concentration. In this study, we established a cell culture method to simulate the chronic low-concentration FA exposure by using a serial passage strategy. Murine neuroblastoma N2a cells and primary murine hippocampal neurons were exposed to a simulated pathological FA concentration referred to AD patients. During the long-term of culture, FA gradually accumulated in the medium and impaired N2a cells. High performance liquid chromatography, cell viability assay and lactate dehydrogenase assay showed that, the FA-elimination capacity of N2a cell decreases with the incubation time, accompanied with inhibition of cell growth and increase in cell death. Holographic microscopy showed that long-term simulated pathological FA exposure attenuated the cells' adhesive morphology. Cells exposed to FA became thicker, exhibiting impairment of neuronal processes. The number of primary neurites in primary hippocampal neurons were reduced by FA exposure, suggesting a decrease in the connectivity between neurons. Formaldehyde accumulation promoted Tau phosphorylation at its Thr181 and Ser396 epitopes, which may be one of the factors leading to decrease in primary neurites. Our findings indicate that accumulation of simulated pathological concentration of FA impairs neurons, induces Tau hyperphosphorylation and decreases neural connectivity, which would lead to neural dysfunction and eventually contribute to the pathogenesis of age-related cognitive impairment.

**Key words** formaldehyde, cell viability, neural connectivity, tau hyperphosphorylation, cell morphology

**DOI:** 10.16476/j.pibb.2017.0062

Chronic formaldehyde (FA) exposure leads to impairment of human memory<sup>[1-2]</sup>. The concentration of endogenous (urine) FA is positively correlated with the severity of cognitive impairments in patients<sup>[3-4]</sup>. The urine FA level could indirectly indicate the formaldehyde level in brain tissues because FA can easily cross the blood-brain barrier<sup>[5-6]</sup>. The average pathological concentration of FA in the urine of Alzheimer's disease (AD) patients is  $(13.70 \pm 5.17) \mu\text{mol/L}$ , *i.e.*, the pathological FA concentration for AD, which is  $\sim 1.4$  times for the physiological urine FA concentration  $((9.61 \pm 2.90) \mu\text{mol/L})$  in age-matched normal participants<sup>[7]</sup>.

Intentional ingestion of high concentration of FA

leads to a decline in the neuropsychological integrity of animals. Rats injected with FA (0.5 mmol/L) exhibited cognitive deficits in the Morris water maze and led to acute and chronic long-term potentiation impairments<sup>[8]</sup>. Higher concentrations of FA rapidly induce cell death, which is not suitable for the

\*This work was supported by grants from National Basic Research Program of China (2012CB911004) and The National Natural Science Foundation of China (31270868, 31200601).

\*\*These authors contributed equally to this work.

\*\*\*Corresponding author.

YI Fa-Ping. Tel: 86-23-68485991, E-mail: fazicq@163.com

HE Rong-Qiao. Tel: 86-10-64889876, E-mail: herq@ibp.ac.cn

Received: April 17, 2017 Accepted: June 14, 2017

observation of the long-term cellular effect. N2a cells treated with 0.5 mmol/L FA for 24 h decreased to 60% viability after 24 h<sup>[5]</sup>. SH-SY5Y cells incubated in the presence of FA(0.3 mmol/L) for 24 h showed a decrease in cell viability to 75%<sup>[9]</sup>. However, age-related cognitive impairment, for instance AD, is a chronic, progressive and irreversible neurodegeneration. To study the relationship between FA and age-related cognitive impairment, the FA concentrations used in the previous reports were higher than the physiological and pathological concentrations of endogenous FA in aging people. Therefore, the long-term cellular effects of exposure to low concentrations of FA, consistent with the pathological FA concentration, should be investigated.

Cognitive function depends upon the connectivity between neurons and the established neural circuit<sup>[10]</sup>. Impairment of neural circuit is closely related with neurodegenerative diseases, for instance AD<sup>[11]</sup>. Neurites are involved in synaptic plasticity<sup>[12]</sup> and formation of neuronal networks<sup>[13]</sup>. Impairment of neurites or neuronal processes leads to the disturbance in the connections between neurons, and thus affects the neural plasticity. Lu and colleagues<sup>[5]</sup> have observed the atrophy of neuronal processes of N2a cells in the presence of high concentrations of FA (0.5 mmol/L) in a short-term culture. Later, Yu and coworkers<sup>[4]</sup> have confirmed the same phenomenon. However, whether pathological concentration of FA can induce atrophy of neuronal processes and neurites during a long-term culture remains elusive.

Tau, one of the important microtubule associated proteins is distributed in cytoplasm and neurites<sup>[14-15]</sup>. This protein promotes the assembly of microtubule and stabilizes cellular skeleton system of neurons, functioning in synaptic plasticity and cognitive dysfunction<sup>[16]</sup>. Hyperphosphorylation of Tau leads to disruption of microtubule system and neural plasticity<sup>[17]</sup>. As described previously, FA is capable of inducing Tau phosphorylation at T181 and S396, subsequently leading to cell death through activation of glycogen synthase kinase-3 beta (GSK-3 $\beta$ ) and calmodulin-dependent protein kinase II (CaMK II)<sup>[5, 18-21]</sup>. The phosphorylation of Tau at T181 and S396 peaked at 4 h of exposure to FA (0.5 mmol/L), gradually decreased from 4 h to 8 h and then increased again from 8 h to 12 h during the culture<sup>[5]</sup>. Treatment with 0.2 mmol/L FA induced cell death and increased Tau hyperphosphorylation at T181 and S396 in SH-SY5Y

cell<sup>[9]</sup>. The detrimental component of methanol toxicity in the methanol-fed mice caused hippocampal Tau phosphorylation and the subsequent impaired memory<sup>[22]</sup>. However, whether long-term exposure to a pathological concentration of FA could increase Tau hyperphosphorylation and subsequently lead to cell death is unclear.

As described previously in our work<sup>[7]</sup>, we re-analysed the clinical investigated data (Figure S1). In the present study, the concentration of FA employed was based on the average values in AD patients and normal ageing participants. We established a cell culture system with long-term treatment with a low concentration of FA to simulate the chronic exposure to the FA concentration of AD patients who were in hospital. The response of N2a cells to the low concentration FA exposure was examined. We found that low concentration of FA accumulation decreased viability, followed by alterations in cell morphology and Tau hyperphosphorylation. We provide novel evidence to support that long-term exposure to a simulated pathological concentration of FA would induce impairment of neurites and neuronal processes, Tau hyperphosphorylation and cell death.

## 1 Materials and methods

### 1.1 Cell culture and accumulation of simulated pathological concentration of FA

Murine neuroblastoma Neuro-2a cells (China Cell Resource Confederation, Beijing, China) were maintained in DMEM-F12 (Corning, USA) supplemented with 10% (*v/v*) fetal bovine serum (FBS; PAA Laboratories, Austria) as monolayers in petri dishes (Corning, USA), at 37°C and 5% CO<sub>2</sub> with > 95% relative humidity. Unless stated otherwise, cells were enzymatically digested (0.25% trypsin, Gibco/Invitrogen, USA; and 0.025% ethylene diamine tetraacetic acid, EDTA; in phosphate buffered saline, PBS; pH 7.2) and passaged every two days.

To evaluate the effect of exposure to a pathological dose of FA in N2a cells<sup>[5, 23]</sup>, cells were maintained in the cell culture medium with the presence of a low concentration of FA(Sigma-Aldrich, USA) by a serial passage strategy. We simplified and called pathological concentration instead of the simulated pathological concentration unless stated otherwise. To simulate the chronic exposure to accumulation of the pathological dose of FA, cells were seeded into 100 mm petri dishes at  $5 \times 10^5$  cells/ml

in 8 ml of cell culture medium ( $4 \times 10^6$  cells), which was supplemented with  $10 \mu\text{mol/L}$  FA (FA-medium). Inoculated and fresh cell culture media were collected. Cells were passaged daily for the following 6 days. The conditional FA-medium was collected before the

passaging. After trypsinization, aliquots of cell samples were harvested, and  $4 \times 10^6$  cells were seeded into a new 100 mm petri dish with 8 ml of FA-medium (Figure 1). The control cells were serially passaged in cell culture medium without the addition of FA.

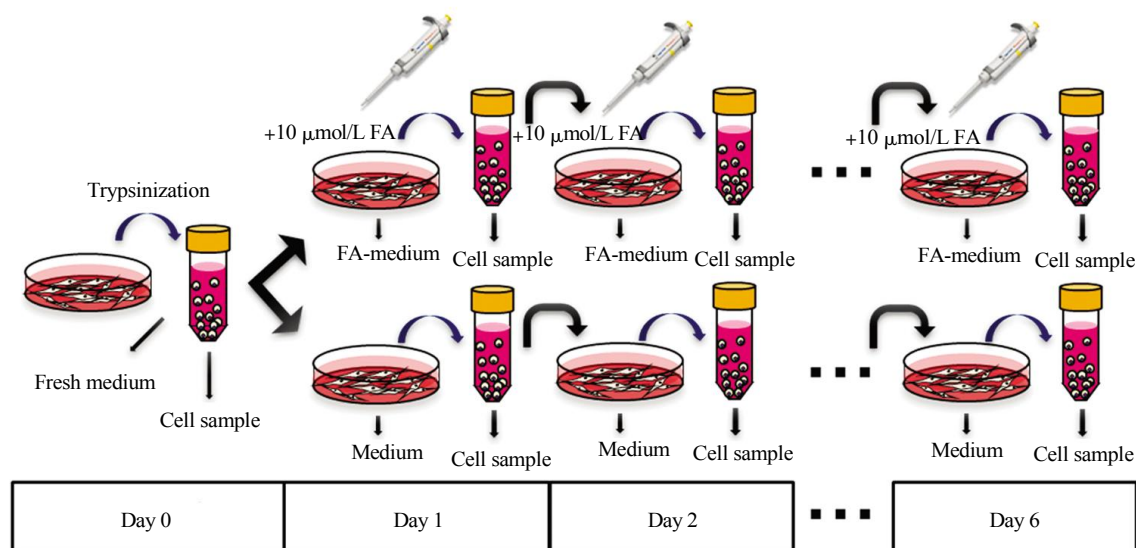


**Fig. 1** The schematic diagram of the serial passages of cell culture in the presence and absence of FA

Neuro-2a (N2a) cells were inoculated at a seeding density of  $5 \times 10^5$  cells/ml and cultured in the presence of FA (final concentration,  $10 \mu\text{mol/L}$ ) for 24 h, after which aliquots were taken for another inoculation at the same seeding density and in the presence of the same concentration of FA. Then, this culture procedure was continued until the end of day 6. Aliquots were taken each day for the analysis as indicated.

## 1.2 Primary culture of hippocampal neuron

Primary fetal hippocampal neurons were isolated from 18-day pregnant C57BL/6 mice, as described previously<sup>[24]</sup>. In brief, hippocampi were dissociated by trypsinization and trituration and the dissociated cells were plated into 12-well plates at  $1.8 \times 10^4$  cells/cm<sup>2</sup> on poly-D-lysine-coated glass coverslips. Cultures were maintained in the neuron culture medium: neurobasal medium (Gibco, USA) with 2% B27 supplement (Gibco, USA), 1% glutamax (Gibco, USA) and 1% pen/strep (Gibco, USA). Cultures were then fed with 1/2 media changes every three days (remove 0.5 ml and add 1 ml) to protect against media evaporation and metabolic by product accumulation. Primary cultured neurons were used for plasmid transfection after 13 days incubation (13 DIV).

## 1.3 Primary neurite assay

Primary cultured neurons were transfected with pEGFP-N1 plasmid (a kind gift from Prof. LI Guo-Dong, Institute of Biophysics, Chinese Academy

of Sciences) using lipo2000 (Invitrogen, USA) for 3 h on 13 DIV and then the medium was changed with fresh neuron culture medium. The transfected neurons were treated with FA the next day, as described above. In these experiments, pEGFP-N1 and lipo 2000 were mixed at a mass: volume ratio of  $1 \mu\text{g} : 1 \mu\text{l}$ . Images of cultured hippocampal neurons were obtained after three days incubation with a confocal microscope system (FV1200; Olympus, Japan) equipped with a  $20 \times \text{NA}1.3$  lens using FV1200. The morphology of neuron was analysed with the ImageJ software. The number of the primary neurites was determined.

## 1.4 Ultraviolet high-performance liquid chromatography (UV-HPLC)

The concentration of FA in cell culture medium was measured by UV-HPLC. In brief, 0.5 ml of 10% trichloroacetic acid (Xilong Chemical Co., Ltd., USA) was added to 1 ml of cell culture medium prior to centrifugation ( $12\,000 \text{ r/min}$ ,  $4^\circ\text{C}$ , 30 min). The supernatants (0.4 ml) were pipetted into 1.5-ml

Eppendorf tubes and mixed with 0.5 ml of acetonitrile (HPLC-grade purity, Fisher Scientific, USA) and 0.1 ml of 2, 4-dinitrophenylhydrazine (DNPH; Beijing Chemical Reagent Research Institute, Beijing, China). Next, the samples were centrifuged (12 000 r/min, 4°C, 10 min), incubated in a 60°C water bath for 30 min, and centrifuged again (12 000 r/min, 4°C, 10 min). The FA concentration was determined *via* HPLC (Shimadzu, Japan) as described previously<sup>[25]</sup>.

### 1.5 Cell viability assay

Cell viability was measured by a CCK-8 kit (Beyotime, China). In brief, cells were seeded into 96-well plates at a concentration of  $1 \times 10^4$  cells per well and treated with 10  $\mu\text{mol/L}$  FA as described above. 24 h later, the CCK-8 reagent was added. Plates were incubated at 37°C for 1 h, and the absorbance was recorded at 450 nm by a plate reader (Molecular Devices, USA)<sup>[5]</sup>.

### 1.6 Lactate dehydrogenase (LDH) assay

Cytotoxicity was measured by an LDH cytotoxicity assay kit (Beyotime, China). In brief, cells were seeded into 96-well plates at  $4 \times 10^4$ /well and exposed to 10  $\mu\text{mol/L}$  FA for 24 h. Cells grown in the medium-without FA were used as the control. The LDH reagent was added (1 : 100) and incubated at 37°C for 1 h. Then, 120  $\mu\text{l}$  of medium from each well was transferred into a new 96-well plate, and the absorbance was recorded at 490 nm by a plate reader (Molecular Devices, USA).

### 1.7 Digital holographic microscopy

Cell morphology was measured by using digital holographic microscopy. Aliquots were taken for the measurements on morphological parameters by a holographic imaging system (Phase Holographic Imaging AB, Sweden) as previously described<sup>[26]</sup>. For holographic time-lapse microscopy, the HoloMonitor M3 digital holographic microscope captured 3D information from N2a cells (inoculated at  $5 \times 10^5$ /ml) treated with 10  $\mu\text{mol/L}$  FA. Holograms were digitally captured every 30 min. The thickness ( $T$ ), area ( $A$ ) and volume ( $V$ ) of the cells were recorded. The thickness value ( $T'$ ) was adjusted using the cubic root of the cell volume in order to describe the cell adhesive capacity:  $T' = T/\sqrt[3]{V}$ . The holograms were analysed by using the Hstudio M3 software (Phase Holographic Imaging AB, Sweden).

### 1.8 Western blotting

The lysate proteins were extracted from the N2a cells incubated in the presence and absence of

10  $\mu\text{mol/L}$  FA, as described above. After the indicated incubation time, the growth medium was removed by aspiration, and each well was washed twice with 1 ml of PBS. The total protein were harvested in ice-cold SDN buffer (Beijing Cell chip Biotechnology, Beijing, China) containing a phosphatase and protease inhibitor (1 mmol/L PMSF). Protein samples for SDS-PAGE were prepared, as described previously<sup>[27]</sup>. After SDS-PAGE, the proteins were transferred to PVDF membranes and the PVDF membranes were incubated with primary antibodies of Tau (1 : 1000 dilution, Millipore, USA), p-T181 (1 : 1000, SBA, USA), p-S396 (1 : 1000; Invitrogen, USA) and  $\beta$ -actin (1 : 2000, Santa Cruze, USA)  $\beta$ -actin was used as loading control. The immunoreactive bands were visualized after exposure of the membranes to Kodak X-ray film.

### 1.9 Immunofluorescence staining

Immunofluorescence staining were performed as previously described<sup>[5]</sup>. In brief, N2a cells were fixed in 4% paraformaldehyde for 10 min. After fixation, cells were incubated in 0.1% Triton X-100 at 4°C for 10 min and then washed 3 times in PBS for 5 min each. Cells were incubated in PBS with 10% normal goat serum at room temperature for 30 min and then incubated in primary antibodies p-T181 or p-S396 overnight at 4°C. The specimens were incubated with biotin-labelled secondary antibodies (37°C, 1 h) after washed 3 times with PBS and the images was obtained by microscopy (Leica, Germany).

### 1.10 Statistical analysis

Data were shown as means  $\pm$  standard error mean (s.e.m.) of at least three independent experiments, unless otherwise stated. Means were compared using one-way ANOVA, unless otherwise stated. The distribution of primary neurite number was analysed by Chi-square test. Significance was accepted at  $P < 0.05$ .

## 2 Results

### 2.1 Accumulation of pathological FA declines cell viability and induces cell death

The baseline FA concentration in the control medium (without FA) was stabilized at  $(5.12 \pm 0.81)$   $\mu\text{mol/L}$  during the 6-day incubation period (Figure 2a). Therefore, 10  $\mu\text{mol/L}$  FA was supplemented into the cell culture medium (FA-medium) to mimic the pathological concentration of FA ( $\sim 15$   $\mu\text{mol/L}$ ), based on our previous measurements on the uric FA level in AD patients<sup>[7]</sup> (Figure S1). N2a cells were

maintained in the FA-medium for 6 days by a serial passage procedure (Figure 1). The HPLC assay showed that the FA concentration in the daily collected FA-medium gradually increased from  $\sim 6 \mu\text{mol/L}$  (day 1) to  $\sim 11 \mu\text{mol/L}$  (day 6), showing accumulation of

formaldehyde (Figure 2a). Thus, N2a cells could eliminate the excessive FA in the medium, which can be attributed to the metabolism of FA by N2a cells; however, the capacity to eliminate FA decreased with increasing duration of exposure to FA.

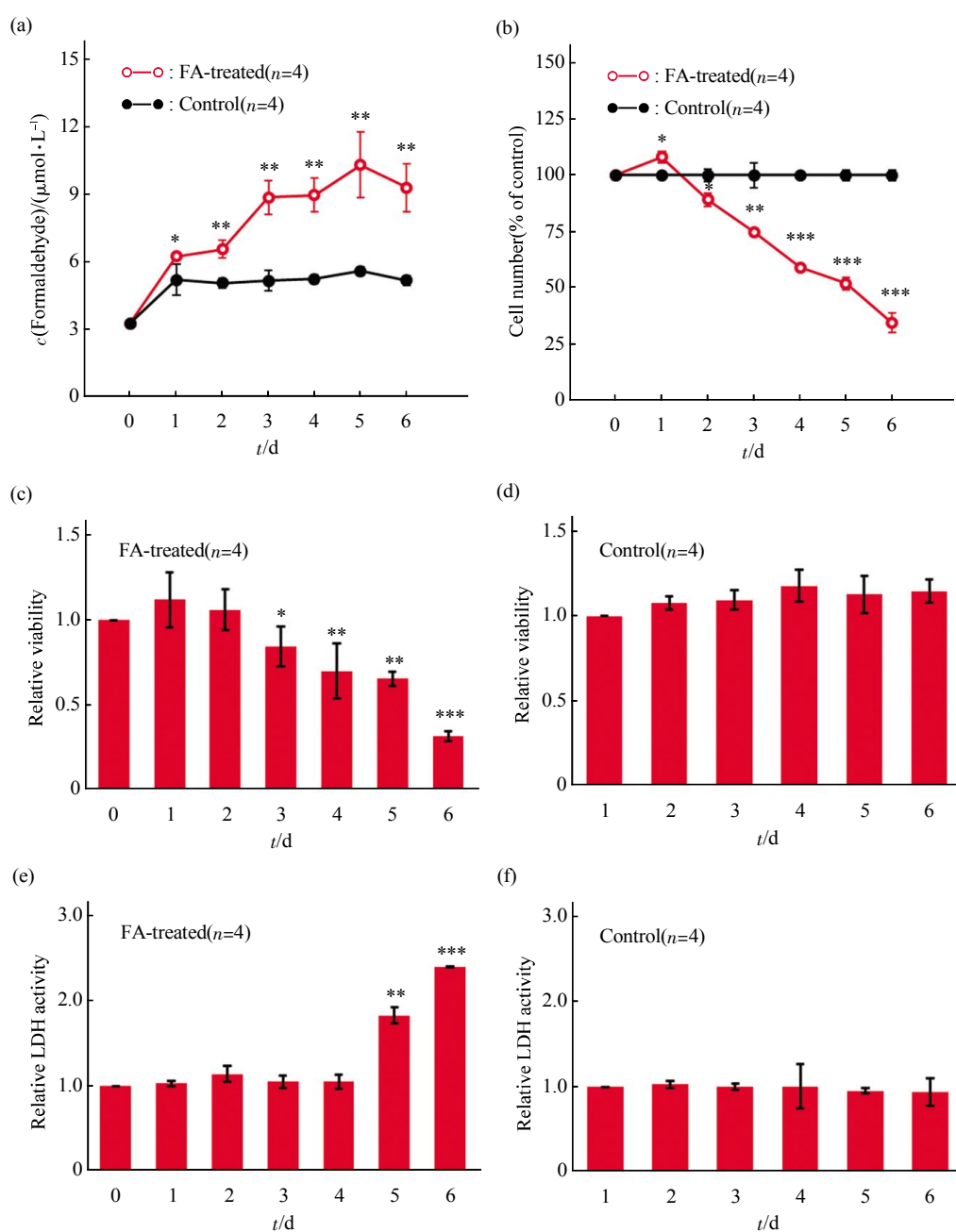


**Fig. 2** Effects of long-term pathological FA (10  $\mu\text{mol/L}$ ) exposure on N2a cell

N2a cells were cultured and inoculated as described for Figure 1. The concentration of FA in the medium gradually accumulated when cells were grown in the presence of FA while the concentration of FA in the medium of control cells maintained stable at the base line level (a). The relative number of the FA-treated cells dramatically dropped down along the incubation time as compared with the control cells (b). The viability of the FA-treated cells also decreased along the incubation time (c) but the viability of the control cells remained unchanged (d). The activity of released LDH in the conditional medium from the FA-treated cells increased at day 5 and day 6 (e) while that in the conditional medium from the control cells remained unchanged. The data were from a representative experiment.  $n$  is the number of parallel samples. Data were shown as mean  $\pm$  S.D. Means were compared by Student's  $t$ -test. \* $P < 0.05$ ; \*\* $P < 0.01$ ; \*\*\* $P < 0.001$ .

Along with the decrease in FA-elimination capacity, FA-induced decrease in cell number was also recorded. The number of cells increased ( $P < 0.05$ ) at day 1 but gradually decreased in the following days (Figure 2b). The number of the FA-treated cells was fewer than 50% of the control cells after 6-day incubation. The CCK-8 assay confirmed the FA-induced decrease in cell viability with increasing duration of FA treatment (Figure 2c). The viability of FA-exposed cells was significantly decreased ( $P < 0.05$ ) at day 3 and was only  $\sim 25\%$  of the day 0 cells ( $P < 0.001$ ) at day 6. The viability of control cells was maintained at a stable level during the 6-day incubation period (Figure 2d). FA-induced cell damage was measured *via* the LDH assay. Although, the LDH activity in the medium was not changed from day 1 to day 4, the decrease in cell number and cell viability from day 1 to day 4 suggested that the leakage of LDH per cell was increased. The LDH leakage markedly increased ( $P < 0.01$ ) at day 5 and day 6, indicating elevated cell death in the FA-exposed cells later in the exposure period (Figure 2e). Meanwhile, we did not detect the increase of LDH activity in the control medium, indicating that no cell death occurred in the control cells (Figure 2f). These results indicate that long-term exposure to low-concentration FA ( $10 \mu\text{mol/L}$ ) decreases cell viability and induces cell death, especially at the later incubation period (from day 4 to day 6), when the FA-elimination capacity has been significantly inhibited.

## 2.2 Long-term pathological FA exposure weakens the cells' adhesive morphology

Holographic time-lapse microscopy was employed to monitor the changes in the morphology of the FA-exposed cells and the control cells. Cells were passaged daily as described above. During the serial passaging, cells in both the FA-exposed and control conditions became less attachable, as indicated by the increase in the adjusted thickness. In particular, the value of adjusted thickness of the FA-exposed cells was significantly larger ( $P < 0.01$ ) than that of the controls from day 3 to day 5, indicating that the FA exposure weakened the cell adhesion (Figure 3a). The area of the control cells remained stable during the 5-day incubation period. However, the area of the FA-exposed cells decreased at day 3 and day 5

(Figure 3b). The volume of control cells increased later during the incubation period, but the volume of the FA-exposed cells remained stable (Figure 3c). An increase in cellular volume in the FA-exposed cells was recorded at day 1, suggesting that short-term exposure to low concentrations of FA was able to promote the growth of N2a cells, as depicted in Figure 2b. However, the volumes of the control and FA-exposed cells were similar from day 3 to day 5. As shown in Figure S2, cells exposed to FA for 3 days appeared rounder than the controls, similar to the results described above. In addition, phase-contrast bright field imaging showed that 6 days of continuous FA exposure significantly repressed the extension of cell processes, and cells were rounded and aggregated, which was accompanied with a decrease in cell density (Figure 3e). In contrast, N2a cells in the control group adhered to the bottom of the petri dish and spread out and spindle-shaped and maintained a high cell density (Figure 3f). Therefore, N2a cells are sensitive to treatment with low-dose FA at  $10 \mu\text{mol/L}$ . The monitoring of dynamic morphological changes revealed that long-term pathological FA exposure weakens the adhesive morphology of the cells. The FA-induced rounding and inhibition of cell process formation in neuronal cell lines imply that long-term, low-dose pathological FA exposure would likely impair the connections between neurons.

## 2.3 Long-term pathological FA disrupts neurite morphology

To further evaluate the effect of long-term pathological FA on the connections between neurons, we cultured primary hippocampus neurons and compared the neurite morphology between the FA-treated and control neurons. Neurons (13DIV) were treated with  $10 \mu\text{mol/L}$  FA for 3 days. The medium was changed daily. The number of neurites in the FA-treated neurons (Figure 4a) was smaller than that in the control neuron (Figure 4b). The number of neurites in the control neurons averaged  $\sim 6$ . While, the number of neurites of the FA-treated neurons were  $\sim 4$ , significantly smaller ( $P < 0.01$ ) than that of the control (Figure 4c). Therefore, we hypothesized that long-term pathological FA would lead to neural damage by interfering with the morphology and function of neurites.

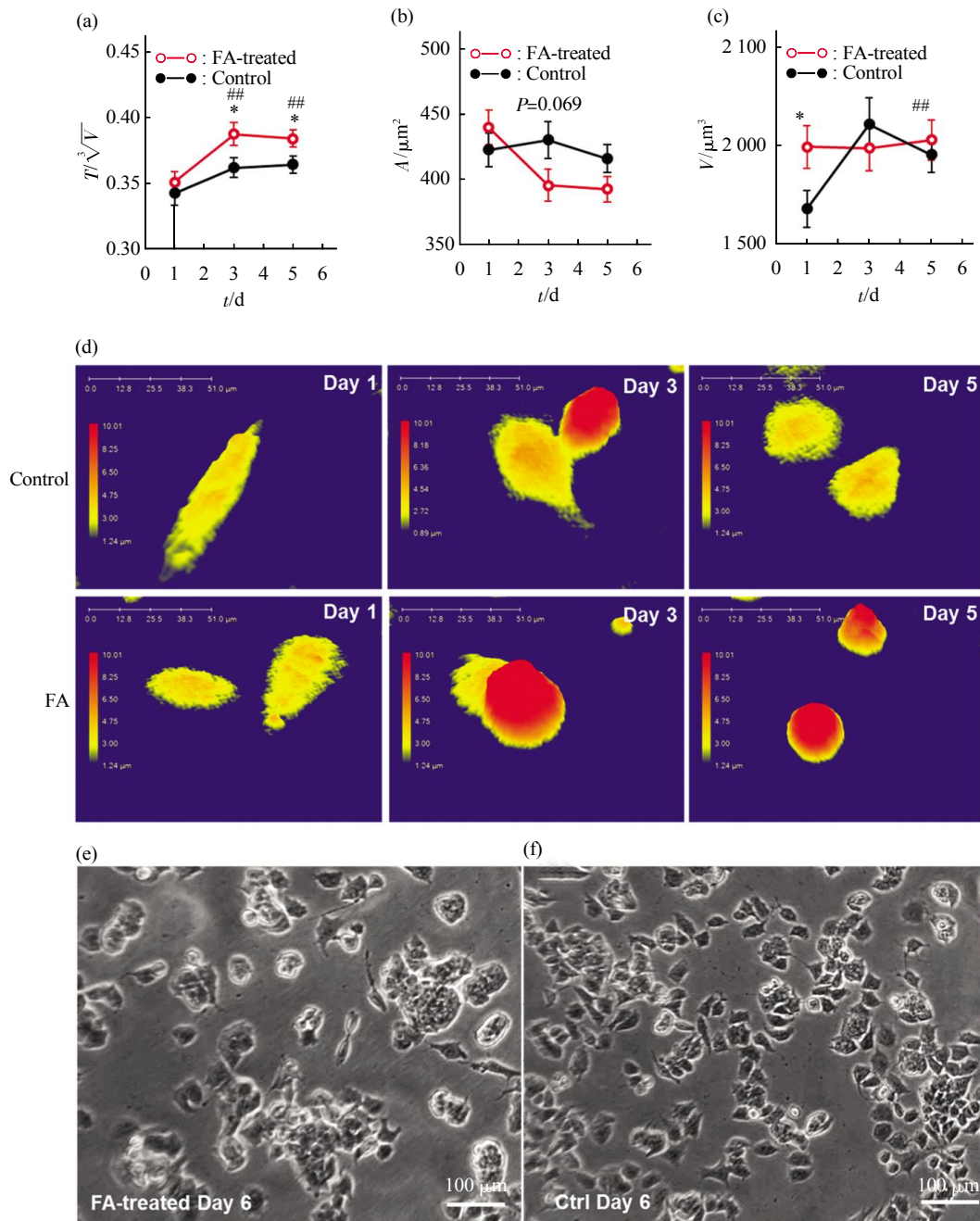


**Fig. 3 Morphological changes of N2a cells in the presence of FA of ~10  $\mu\text{mol/L}$**

Cell culture and inoculation were performed as described for Figure 1. Aliquots of N2a cells were taken on day 1, day 3 and day 5 for the measurements of morphological parameters when cells had adherent to the bottom of the petri dishes, by holographic imaging. The adjusted thickness ( $T/\sqrt[3]{V}$ ) (a), area (b) and volume (c) were compared between the 10  $\mu\text{mol/L}$  FA-treated and control cells. The representative holographic images of the FA-treated and control cells were displayed in panel (d). The representative bright field phase-contrast images of the morphologies of day 6 cells were displayed in panel (e) (FA-treated group) and panel (f) (control group). Data in panel (a)~(c) were obtained from at least three independent experiments. Day 1:  $n = 170$  for FA-treated cells and  $n = 124$  for control cells. Day 3:  $n = 143$  for FA-treated cells and  $n = 163$  for control cells. Day 5:  $n = 198$  for FA-treated cells and  $n = 230$  for control cells. Data were shown as means  $\pm$  s. e. m. Means were compared with one-way ANOVA. The  $P$  value and the asterisks in panel (a)~(c) indicated the mean comparisons between the FA-treated and control cells at each time point. \* $P < 0.05$ ; \*\* $P < 0.01$ ; \*\*\* $P < 0.001$ . The pound signs indicated the comparisons between the means of the FA-treated cells and the means of the control cells at day 1. # $P < 0.01$ ; ## $P < 0.001$ .

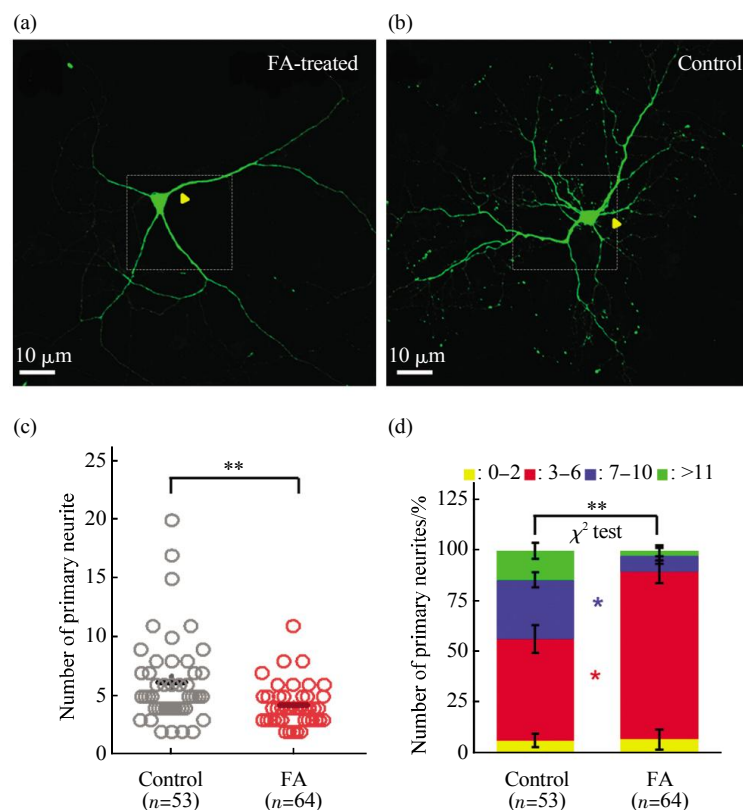


**Fig. 4** Changes in neurites morphology in the presence of FA at the concentration of 10  $\mu\text{mol/L}$

The representative morphology of the neurites of primary hippocampal neurons cultured in the presence of 10  $\mu\text{mol/L}$  formaldehyde (a) and control neurons cultured without the presence of formaldehyde (b) were displayed. The primary neurons were transfected with EGFP plasmid at 13DIV and the transfected neurons were then treated with FA at the concentration of 10  $\mu\text{mol/L}$  for three days. The medium was changed every day. Images of EGFP-positive neurons were observed with fluorescence confocal microscopy. The number of primary neurites was quantified by the ImageJ software. (c) The number of primary neurites of the FA-treated neurons ( $n = 53$ ) was significantly smaller than the control neurons ( $n = 64$ ). (d) The distribution of primary neurites numbers in the FA-treated and control neuron populations differed significantly. The distribution of neurites number was analyzed by Chi-square test. Data in panel (c, d) were collected from three independent experiments. Data are shown as mean  $\pm$  s.e.m. Means were compared with one-way ANOVA. \* $P < 0.05$ ; \*\* $P < 0.01$ .

#### 2.4 Long-term pathological FA exposure leads to Tau hyperphosphorylation

It was established that high concentration of FA leads to cell death by inducing Tau hyperphosphorylation<sup>[5, 21]</sup>. Western blotting showed that the phosphorylation at T181 and S396 increased along with the incubation time (from day 0 to day 6) in the FA-exposed cells (Figure 5a) but the level of p-T181 and p-S396 was stable in the control cells

(Figure 5b). Immunofluorescence staining confirmed that the number of cells positive for p-T181 and p-S396 (red) increased with incubation time in the FA-exposed group (Figure 5c). Under the experimental conditions, cells in the absence of FA showed no significant changes in Tau phosphorylation. All of these results demonstrated that long-term pathological FA exposure increased the level of Tau phosphorylation.

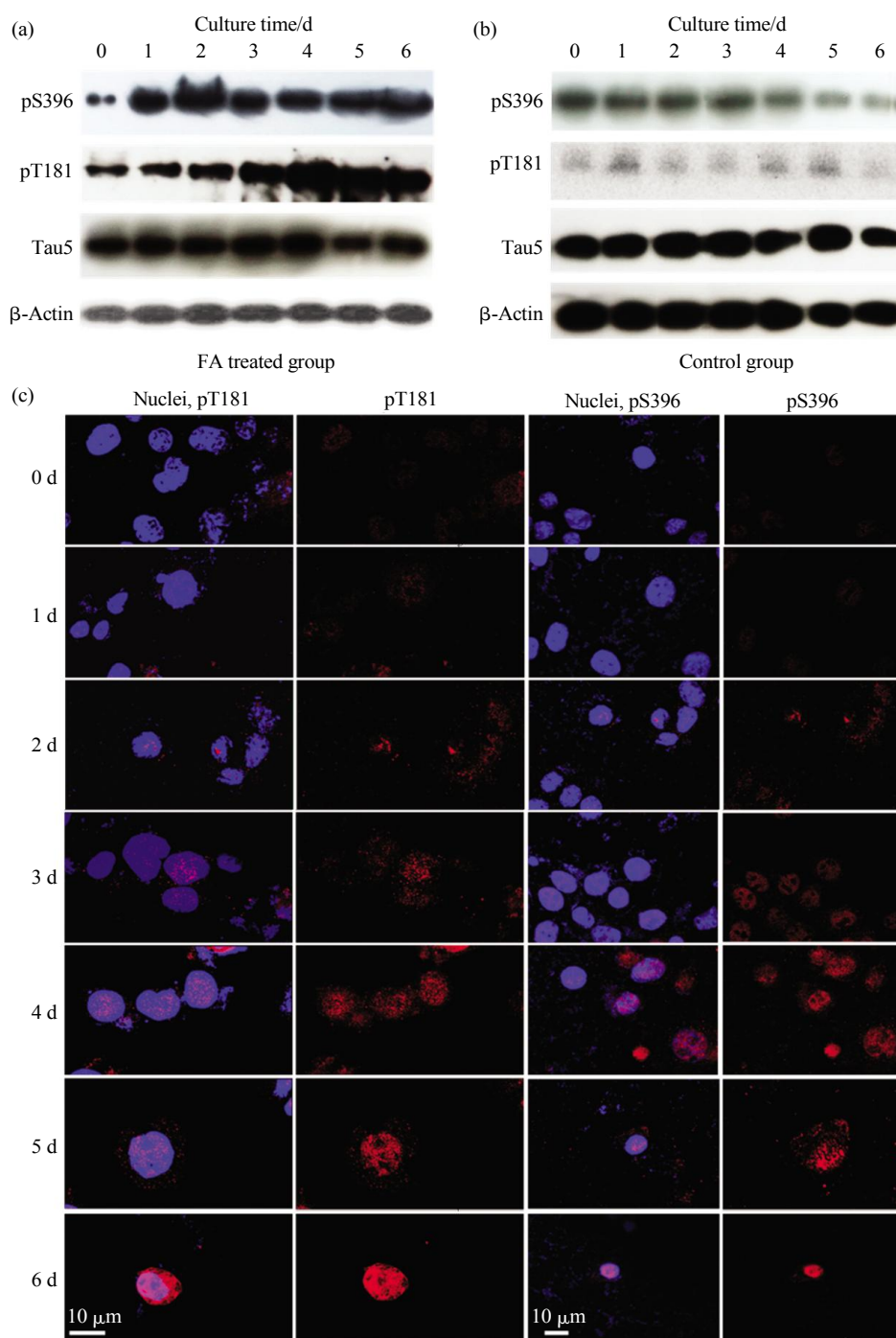


**Fig. 5 Changes in the phosphorylation of Tau protein in N2a cells in the presence of FA**

Cell culture conditions were as described for Figure 1. The phosphorylation of Tau protein in N2a cells treated with 10 μmol/L FA (a) and in N2a control cells that were cultured without the presence of FA (b) from day 0 to day 6 was detected *via* Western blotting with anti-p-S396 and anti-p-T181 (a). Immunofluorescence staining of phosphorylation of Tau protein (c) with anti-p-S396 (red) and anti-p-T181 (red) was carried out in N2a cells in the presence of FA from day 0 to day 6.

### 3 Discussion

In this paper, we show that a concentration of FA based on the pathological level in AD patients could repress cell viability, induce cell death, weaken cell adhesion and increase the level of Tau phosphorylation in N2a cells during the long-term cell culture with persistent FA exposure in a novel serial-passage culture strategy. Although accumulation of FA damages neurons *in vitro* and *in vivo*, the FA concentration used in most previous studies were higher than the pathological FA level<sup>[5, 9, 28]</sup>. In fact, the elevation of endogenous FA during ageing is a rather late process. High-concentration FA induces immediate toxic effects on neuronal cells, which cannot reflect the action of FA in the actual pathogenesis *in vivo*. The accumulative toxicity of low-concentration FA in this work provides evidence to support the hypothetic cytotoxicity of a chronic increase in endogenous FA. This is helpful for understanding the age-related cognitive impairment with abnormal FA elevation<sup>[3-4]</sup>.

As the fresh cell medium contains  $\sim 5 \mu\text{mol/L}$  FA, we added  $10 \mu\text{mol/L}$  to the cell culture medium to mimic a pathological FA concentration at the beginning of the experiment. However, in practice, the FA concentration in the medium was lower than the expected level. These results suggest that cells likely increase the FA degradation process in order to eliminate the excess FA in the environment, which may be a self-protection function of cells in response to a mild FA exposure. Many studies have shown that herbal medicines protect cells against the FA-induced apoptosis by reducing the FA level in the medium as well<sup>[9, 29]</sup>. However, such defensive responses cannot be sustained for a long time when the environmental FA level is deliberately maintained in excess. Our serial passage procedure can maintain a relatively long-term incubation of cells with a low concentration of FA. It successfully established an accumulation of pathological concentration of FA in the cell culture. We have got a chance to observe the impairment of neural cells under the pathological concentration of FA, referred to the AD patients on clinical.

Silent synapsis is one of the pathological changes in the early onset of AD<sup>[30]</sup>, which is closely related with changes in connectivity between neurons<sup>[31]</sup>. Therefore, we observed the dynamic morphological changes in the FA-exposed cells along with the serial

passages in order to capture the real-time action of FA on N2a cells. In the holographic imaging experiment, cells were serially passaged as described in Figure 1, except that the morphological information was obtained during the initial cell adhesion process rather than after 1 day of FA exposure. Here, accumulation of pathological concentration of FA suppresses neurites and neuronal processes indicating that formaldehyde could play a role in disturbance of the connections between neurons, which is related to silent synapsis. This viewpoint is based on these observations as follows. (1) In the long-term pathological FA treatment, N2a cells became round and atrophic and less attached to the bottom of the petri dish (Figure 3). (2) The hippocampal neurons possessed fewer cellular processes compared with the control cells. These data suggests that the low concentration of FA might chronically inhibit the connections between neurons through diminishing the neurites and neuronal processes.

Tau protein plays an important role in the formation and maintenance of axons and dendrites (neurites)<sup>[32]</sup>, through promotion and stabilization of the microtubule system and actin filaments<sup>[33-36]</sup>. The function of Tau is regulated by phosphorylation and dephosphorylation. When it is hyperphosphorylated, Tau will disassociate off microtubules and actin filaments, followed by the disruption of the cytoskeleton. In this work, long-term treatment with pathological concentration of FA resulted in Tau hyperphosphorylation at T181 and S396. Tau hyperphosphorylation could disassociate off microtubule system, leading to disruption of neuronal processes and neurites.

Changes in the viability and number of cell progressed in three stages. First, the cell number was promoted by low concentration of FA in 24 h (Figure 2b). This phenomenon has been reported by several laboratories<sup>[37-38]</sup>. Second, however, from day 2 to day 4, cell growth was inhibited, resulting in the decrease of cell viability. At this stage as shown in Figure 2a, the FA concentration accumulated in the medium accompanied with the increase of cytotoxicity, which subsequently impaired the neuronal processes and disturbed the cell adhesion capacity (Figure 3 and 4). Third, from day 5 to day 6, cell death occurred because LDH was markedly released into the culture medium (Figure 2e). According to Giordano and colleagues<sup>[39]</sup>, dying cells release LDH in the medium whose

quantification is proportional to the number of dead cells. Therefore, the gradual decrease of the total cell number could be attributed to the inhibition of cell growth from day 2 to day 4, and then to cell death at last two days, except for the promotion of cell proliferation on day 1.

Accumulation of FA cytotoxicity could be an explanation for the phenomenon that the cell number gradually decreased on the following days. FA exposure promotes cellular oxidative stress as described by Jung and coworkers<sup>[40]</sup>. In this laboratory, it was also observed that addition of FA to cells markedly promotes the production of ROS<sup>[41-42]</sup>, so called FA stress<sup>[43]</sup>. According to Zerlin and colleagues<sup>[44]</sup>, FA exposure induces oxidative stress, mitochondrial dysfunction and apoptosis. Oxidative stress plays a key role in age-related cognitive impairment<sup>[45-46]</sup>. The intestinal microbiota is an important source of endogenous FA for the APP/PS1 transgenic mouse<sup>[47]</sup>. In this work, the medium was replaced each day by fresh FA-medium to maintain the FA concentration in the cell culture medium. FA exposure was continued and the oxidative stress was chronically maintained to the cells even though the pathological concentration of FA was used.

Tau hyperphosphorylation was markedly observed during the culture. At first, phosphorylation of Tau acted as a cellular response to the formaldehyde stress. As described by Wang and colleagues<sup>[48]</sup>, Tau hyperphosphorylation could have neuroprotective effects on neurons as an early stage of cellular response to oxidative stress. However, when the oxidative stress is maintained and prolonged, Tau hyperphosphorylation will be accumulated in cells, which could become cytotoxic to neurons. Recently, Tau pathology was regarded as an important risk factor to induce excitatory neuron loss, grid cell dysfunction, and spatial memory deficits reminiscent of early AD<sup>[49]</sup>. This may be another explanation for changes in cell number in the presence of low concentration of formaldehyde under the conditions we used.

We treated N2a cells for 6 days with low concentration of FA, which is based on the average concentrations of urine FA in both AD patients and normal participants but not on the blood or brain concentrations of FA. The reasons may be as follows: (1) Urine FA comes from blood, which permeates through kidney. (2) FA is active in reactions with amino groups, such as proteins. Blood proteins

markedly disturb the reaction of DNPH with FA and result in large errors in the experiments. (3) In contrast, urine contains very little protein and does not remarkably interfere with the reaction of DNPH with FA. The data are more consistent and repeatable from urine FA determination. (4) Although we have analysed the concentration of brain FA<sup>[5]</sup>, we cannot be sure whether the values result simply from the reaction between DNPH with FA, because brain tissues are much more complicated than blood or urine. Finally, (5) FA can pass through the blood brain barrier<sup>[5]</sup>; thus, uric data might indirectly represent the FA in brain tissues. Thus, we used the average value of urine FA. However, we should develop a new method to determine the concentration of brain FA more accurately in the future.

Taken together, we demonstrated that the accumulation of pathological concentration of endogenous FA is able to induce chronic damage to N2a cells, especially the impairment of neuronal processes and neurites, which may be resulted from Tau hyperphosphorylation.

**Acknowledgements** We thank MIAO Jun-Ye (Institute of Biophysics, Chinese Academy of Sciences) for her kind assistance and advice on the experiments. We thank Mr. HU Ping-Dong for his kind assistance in the plasmid transfection experiment.

**Supplementary material** Figures S1 – S2 are available at paper online(<http://www.pibb.ac.cn>).

## References

- [1] Kilburn K H. Neurobehavioral impairment and seizures from formaldehyde. *Arch Environ Health*, 1994, **49**(1): 37–44
- [2] Tong Z, Han C, Luo W, *et al.* Accumulated hippocampal formaldehyde induces age-dependent memory decline. *Age*, 2013, **35**(3): 583–596
- [3] Tong Z, Zhang J, Luo W, *et al.* Urine formaldehyde level is inversely correlated to mini mental state examination scores in senile dementia. *Neurobiol Aging*, 2011, **32**(1): 31–41
- [4] Yu J, Su T, Zhou T, *et al.* Uric formaldehyde levels are negatively correlated with cognitive abilities in healthy older adults. *Neurosci Bull*, 2014, **30**(2): 172–184
- [5] Lu J, Miao J, Su T, *et al.* Formaldehyde induces hyperphosphorylation and polymerization of Tau protein both *in vitro* and *in vivo*. *Biochim Biophys Acta*, 2013, **1830**(8): 4102–4116
- [6] Shcherbakova L N, Tel'pukhov V I, Trenin S O, *et al.* Permeability

- of the blood-brain barrier to intra-arterial formaldehyde. *Biull Eksp Biol Med*, 1986, **102**(11): 573-575
- [7] Li T, Su T, He Y, *et al.* Brain formaldehyde is related to water intake behavior. *Aging Dis*, 2016, **7**(5): 561-584
- [8] Tong Z, Han C, Luo W, *et al.* Accumulated hippocampal formaldehyde induces age-dependent memory decline. *Age (Dordr)*, 2013, **35**(3): 583-596
- [9] Song Y X, Miao J Y, Qiang M, *et al.* Icaritin protects SH-SY5Y cells from formaldehyde-induced injury through suppression of Tau phosphorylation. *Chin J Integr Med*, 2016, **22**(6): 430-437
- [10] Antic S D, Empson R M, Knöpfel T. Voltage imaging to understand connections and functions of neuronal circuits. *J Neurophysiol*, 2016, **116**(1): 135-152
- [11] Busche M A, Konnerth A. Impairments of neural circuit function in Alzheimer's disease. *Philos Trans R Soc Lond B Biol Sci*, 2016, **371**(1700)
- [12] Buffington S A, Huang W, Costa-Mattioli M. Translational control in synaptic plasticity and cognitive dysfunction. *Annu Rev Neurosci*, 2014, **37**: 17-38
- [13] Volovitch M, le Roux I, Joliot A H, *et al.* Control of neuronal morphogenesis by homeoproteins: consequences for the making of neuronal networks. *Perspect Dev Neurobiol*, 1993, **1**(3): 133-138
- [14] Su J H, Cummings B J, Cotman C W. Early phosphorylation of tau in Alzheimer's disease occurs at Ser-202 and is preferentially located with in neurites. *Neuroreport*, 1994, **5**(17): 2358-2362
- [15] Liu W K, Dickson D W, Yen S H. Heterogeneity of tau proteins in Alzheimer's disease. Evidence for increased expression of an isoform and preferential distribution of a phosphorylated isoform in neurites. *Am J Pathol*, 1993, **142**(2): 387-394
- [16] Guo T, Noble W, Hanger D P. Roles of tau protein in health and disease. *Acta Neuropathol*, 2017, **133**(5): 665-704
- [17] Ahmed T, Van der Jeugd A, Blum D, *et al.* Cognition and hippocampal synaptic plasticity in mice with a homozygous tau deletion. *Neurobiol Aging*, 2014, **35**(11): 2474-2478
- [18] Hua Q, He R Q. Effect of phosphorylation and aggregation on tau binding to DNA. *Protein Pept Lett*, 2002, **9**(4): 349-357
- [19] Nie C L, Zhang W, Zhang D, *et al.* Changes in conformation of human neuronal tau during denaturation in formaldehyde solution. *Protein Pept Lett*, 2005, **12**(1): 75-78
- [20] Nie C L, Wang X S, Liu Y, *et al.* Amyloid-like aggregates of neuronal tau induced by formaldehyde promote apoptosis of neuronal cells. *BMC Neurosci*, 2007, **8**(9)
- [21] He X, Li Z, Rizak J, *et al.* Resveratrol attenuates formaldehyde induced hyperphosphorylation of Tau protein and cytotoxicity in N2a cells. *Frontier in Neuroscience*, 2016, **10**(598)
- [22] Yang M, Lu J, Miao J, *et al.* Alzheimer's disease and methanol toxicity (part 1): chronic methanol feeding led memory impairments and tau hyperphosphorylation in mice. *J Alzheimers Dis*, 2014, **41**(4): 1117-1129
- [23] K A. Petro C L S. Membrane raft disruption promotes axonogenesis in n2a neuroblastoma cells. *Neurochem Res*, 2009, **34**(1): 29-37
- [24] Komaki R, Togashi H, Takai Y. Regulation of dendritic filopodial interactions by ZO-1 and implications for dendritomorphogenesis. *PLoS One*, 2013, **8**(10): e76201
- [25] Su T, Wei Y, He R Q. Assay of brain endogenous formaldehyde with 2, 4-dinitrophenylhydrazine through UV-HPLC. *Progress in Biochemistry and Biophysics*, 2011, **38**(12): 1171-1177
- [26] Mo W C, Zhang Z J, Wang D L, *et al.* Corrigendum: shielding of the geomagnetic field alters actin assembly and inhibits cell motility in human neuroblastoma cells. *Sci Rep*, 2016, **6**(32055)
- [27] Wei Y, Han C, Wang Y, *et al.* Ribosylation triggering Alzheimer's disease-like Tau hyperphosphorylation *via* activation of CaMK II. *Aging Cell*, 2015, **14**(5): 754-763
- [28] Wong V C, Cash H L, Morse J L, *et al.* S-phase sensing of DNA-protein crosslinks triggers TopBP1-independent ATR activation and p53-mediated cell death by formaldehyde. *Cell Cycle*, 2012, **11**(13): 2526-2537
- [29] Chen J, Sun M, Wang X, *et al.* The herbal compound geniposide rescues formaldehyde-induced apoptosis in N2a neuroblastoma cells. *Sci China Life Sci*, 2014, **57**(4): 412-421.
- [30] Jack C R Jr, Knopman D S, Jagust W J, *et al.* Hypothetical model of dynamic biomarkers of the Alzheimer's pathological cascade. *Lancet Neurol*, 2010, **9**(1): 119-128
- [31] Voigt T, Opitz T, de Lima A D. Activation of early silent synapses by spontaneous synchronous network activity limits the range of neocortical connections. *J Neurosci*, 2005, **25**(18): 4605-4615
- [32] Gordon-Weeks P R. Growth cones: the mechanism of neurite advance. *Bioessays*, 1991, **13**(5): 235-239
- [33] Avila J. Tau phosphorylation and aggregation in Alzheimer's disease pathology. *FEBS Lett*, 2006, **580**(12): 2922-2927
- [34] Weingarten M D, Lockwood A H, Hwo S Y, *et al.* A protein factor essential for microtubule assembly. *Proc Natl Acad Sci USA*, 1975, **72**(5): 1858-1862
- [35] Caceres A, Kosik K S. Inhibition of neurite polarity by tau antisense oligonucleotides in primary cerebellar neurons. *Nature*, 1990, **343**(6257): 461-463
- [36] Drubin D G, Kirschner M W. Tau protein function in living cells. *J Cell Biol*, 1986, **103**(6 Pt 2): 2739-2746
- [37] Kopke E, Tung Y C, Shaikh S, *et al.* Microtubule-associated protein tau. Abnormal phosphorylation of a non-paired helical filament pool in Alzheimer disease. *J Biol Chem*, 1993, **268**(32): 24374-24384
- [38] Swenberg J A, Moeller B C, Lu K, *et al.* Formaldehyde carcinogenicity research: 30 years and counting for mode of action, epidemiology, and cancer risk assessment. *Toxicol Pathol*, 2013, **41**(2): 181-189
- [39] Giordano G, Hong S, Faustman E M, *et al.* Measurements of cell death in neuronal and glial cells. *Methods Mol Biol*, 2011, **758**: 171-178
- [40] Jung W W, Kim E M, Lee E H, *et al.* Formaldehyde exposure

- induces airway inflammation by increasing eosinophil infiltrations through the regulation of reactive oxygen species production. *Environmental Toxicology and Pharmacology*, 2007, **24**(2): 174–182
- [41] 陈茜茜, 苏 涛, 赫英舸, 等. 氧化应激对溶酶体储存与转运甲醛的影响. *生物化学与生物物理进展*, 2017, **44**(6): 486–494(DOI: 10.16476/j.pibb.2017.0050)
- Chen X X, Su T, He Y G, *et al.* *Prog Biochem Biophys*, **44**(6): 486–494(DOI: 10.16476/j.pibb.2017.0050)
- [42] He R. Abnormal lysosome, Formaldehyde Dysmetabolism and age-related cognitive impairment. *Progress in Biochemistry and Biophysics*, 2016, **43**(12): 1197
- [43] He R, Lu J, Miao J. Formaldehyde stress. *Sci China Life Sci*, 2010, **53**(12): 1399–1404
- [44] Zerlin T, Kim J S, Gil H W, *et al.* Effects of formaldehyde on mitochondrial dysfunction and apoptosis in SK N-SH neuroblastoma cells. *Cell Biol Toxicol*, 2015, **31**(6): 261–272
- [45] Evans A M, Fameli N, Ogunbayo O A, *et al.* From contraction to gene expression: nanojunctions of the sarco/endoplasmic reticulum deliver site- and function-specific calcium signals. *Science China Life Sciences*, 2016, **59**(8): 749–763
- [46] Xiong J, Zhu M X. Regulation of lysosomal ion homeostasis by channels and transporters. *Science China Life Sciences*, 2016, **59**(8): 777–791
- [47] Liu K L, He Y G, Yu L X, *et al.* Elevated formaldehyde in the cecum of APP/PS1 mouse. *Microbiology China*, 2017 (DOI: 10.13344/j.microbiol.china.176008)
- [47] Wang J Z, Wang Z H, Tian Q. Tau hyperphosphorylation induces apoptotic escape and triggers neurodegeneration in Alzheimer's disease. *Neurosci Bull*, 2014, **30**(2): 359–366
- [48] Fu H, Rodriguez G A, Herman M, *et al.* Tau pathology induces excitatory neuron loss, grid cell dysfunction, and spatial memory deficits reminiscent of early Alzheimer's disease. *Neuron*, 2017, **93**(3): 533–541.e5

## 病理浓度甲醛的累积导致小鼠神经母瘤 细胞活力及黏附能力下降\*

王 睛<sup>1)\*\*</sup> 周 均<sup>2)\*\*</sup> 莫炜川<sup>2)</sup> 赫英舸<sup>2)</sup> 魏 艳<sup>2)</sup> 赫荣乔<sup>2)\*\*\*</sup> 易发平<sup>1)\*\*\*</sup>

<sup>1)</sup> 重庆医科大学基础医学院生物化学与分子生物学教研室, 重庆 400016;

<sup>2)</sup> 中国科学院生物物理研究所脑与认知国家重点实验室, 北京 100101)

**摘要** 衰老相关的认知损伤, 如阿尔茨海默病(AD), 是一种缓慢、渐进、不可逆的神经退行性疾病。内源(尿)甲醛浓度与AD病人的认知损害程度呈正相关。但是, 在以前研究中所采用的甲醛浓度, 通常高于AD患者和老年人的病理和生理浓度。因此, 研究长时程低浓度(病理浓度)甲醛对神经类细胞的影响, 对于揭示甲醛在AD发生发展过程的作用是非常必要的。本文参照AD患者尿甲醛浓度, 采用每隔24 h连续传代接种加甲醛(10  $\mu\text{mol/L}$ )的方式, 模拟AD病人尿甲醛浓度, 观察长时程甲醛的累积对小鼠神经母瘤细胞(N2a)和原代海马神经元的影响。通过高效液相色谱、细胞活力和乳酸脱氢酶释放检测显示, 随着孵育时间的延长, 培养基内甲醛浓度积累升高, N2a细胞生长受到抑制, 在甲醛孵育的后期, 细胞死亡显著增加。全息成像显示, 长时程病理浓度甲醛的积累, 使细胞厚度增加、面积减小、神经突受损、显著削弱细胞的黏附能力。同样条件下, 小鼠原代海马神经元的一级神经突的数目显著降低, 表明病理浓度甲醛的积累能够削弱神经元之间的连接。免疫印迹和免疫荧光染色显示, 甲醛的累积可以使N2a细胞内Tau蛋白的181位苏氨酸(T181)和396位丝氨酸(S396)磷酸化水平显著上升, 可能是甲醛累积导致的神经突减少和形态改变的因素之一。以上结果证明, 病理浓度甲醛在细胞生存环境中的累积, 可以导致神经细胞损伤, 尤其是神经突的异常改变。本文为探索甲醛代谢失调与老年认知损害之间关系和机制提供了新的启示。

**关键词** 甲醛, 细胞活力, Tau蛋白异常磷酸化, 细胞形态, 阿尔茨海默病

学科分类号 Q2, Q5

DOI: 10.16476/j.pibb.2017.0062

\* 国家重点基础研究计划(973)(2012CB911004)和国家自然科学基金(31270868, 31200601)资助项目。

\*\* 共同第一作者。

\*\*\* 通讯联系人。

易发平. Tel: 86-23-68485991, E-mail: fazicq@163.com

赫荣乔. Tel: 86-10-64889876, E-mail: herq@ibp.ac.cn

收稿日期: 2017-04-17, 接受日期: 2017-06-14

## Supplements

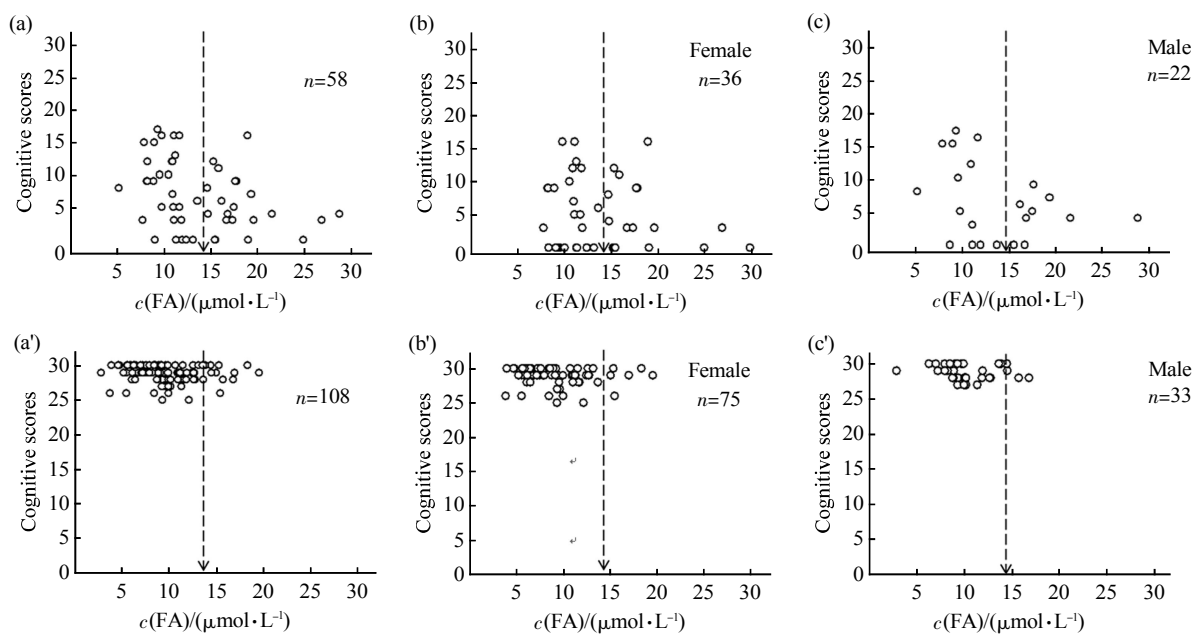


**Fig. S1 Scattering plotting for uric FA and cognitive scores**

The requirements and conditions for the recruit of AD patients and normal participants were as described by Li and colleagues in this laboratory (Li T, Su T, He Y, *et al.* Brain formaldehyde is related to water intake behavior. *Aging Dis*, 2016, 7(5): 561–584), except that the data were reanalyzed with scattering plotting. The MMSE scores and concentrations of uric FA were measured from total AD patients (a), AD female patients (b), male patients (c), total normal participants (a'), female participants (b') and male patients (c'). The dashline represents the average concentrations of FA for AD patients and age-matched normal participants.

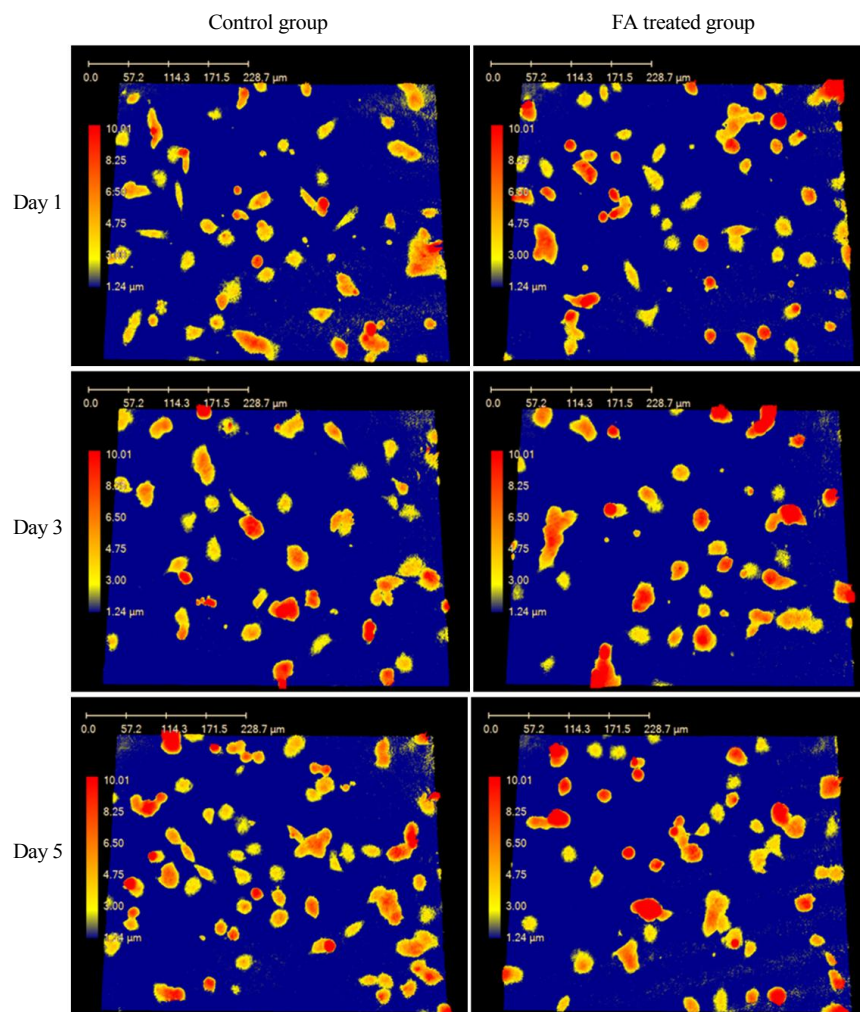


**Fig. S2 Morphological changes in N2a cells in the presence of FA, visualized using real-time holographic imaging**

Cell culture conditions were as described for Figure 1. Aliquots of FA-treated cells were taken (day 1, 3, and 5) as indicated. Cell morphologies in the presence and absence of 10  $\mu\text{mol/L}$  FA were monitored and visualized using real-time holographic imaging.